PHYSICAL REVIEW B VOLUME 37, NUMBER 7 1 MARCH 1988

Ordering in the quenched two-dimensional axial next-nearest-neighbor Ising model

Gregory N. Hassold and David J. Srolovitz
Los Alamos National Laboratory, Los Alamos, New Mexico 87545
(Received 11 June 1987)

Monte Carlo simulations of ordering in the two-dimensional axial next-nearest-neighbor Ising model following a quench were performed using nonconserved dynamics for a wide range of frustration parameters, κ, and temperatures. It was found that in quenches from $T \gg T_c$ to $T < T_c$ for $\kappa \leq 0$ (i.e., in the ferromagnetic regime) ordered domains form quickly and coarsen with the expected $t^{1/2}$ kinetics. Similar results are found for quenches at $\kappa \geq 1$, where the ordered structure is striped. However, for $0 < \kappa < 1$, quenches to low temperature produce a disordered, "glassy" phase, which shows logrithmic ordering kinetics and is insensitive to whether the underlying ground state is ferromagnetic or $\langle 2 \rangle$ phase (i.e., striped phase). Quenches to higher temperatures show the presence of a finite glass-transition temperature. Discontinuous changes in the value of the frustration parameter from the ferromagnetic to the $\langle 2 \rangle$-phase region of the phase diagram at low temperature yields a phase change which occurs via classical nucleation and growth. A simple energetic or growth model is proposed which accounts for all of the temperatures at which the ordering kinetics undergoes transitions.

I. INTRODUCTION

The kinetic evolution of simple spin models (e.g., Ising, Potts) which have been quenched from high temperature ($T \gg T_c$) to a final temperature much less than T_c have been well studied.[1-3] In these simple models the correlation length R generally grows algebraically with time as t^n, where t is time and n is a positive constant. For nonconserved (Glauber) dynamics, n is generally found (theory,[4,5] simulation,[6,7] experiment[5]) to be $\frac{1}{2}$, while for conserved dynamics a theoretical value of $\frac{1}{3}$ is obtained[8] with simulations typically yielding smaller values (see Ref. 1 for a review). Quenches from the paramagnetic region into ferromagnetic regions of the phase diagram generally result in the formation and growth of ordered domains. The domain size distribution[2] and structure factor (see Ref. 1 for a review) are generally found to be time independent when properly scaled.

Natural extensions of the above models can produce systems which exhibit frustration. Probably the simplest frustrated lattice spin model is the nearest-neighbor (NN) antiferromagnetic Ising model on a triangular lattice. In any triangle of nearest-neighbor bonds, at least two of the spins must be identically ordered, thus preventing the satisfaction of the preferred antiferromagnetic bond ordering on every plaquette. Such frustration leads to a disordered ground state. A disordered ground state may also be found in systems with random interactions. Particularly well known in this class is the so called random-field Ising model where frustration is due to the competition between ferromagnetic nearest-neighbor coupling and a spatially varying random magnetic field. Quenches into frustrated regions of the phase diagram generally lead to much slower evolution (subpower law growth) of the correlation length with time.

Since the axial next-nearest-neighbor Ising (ANNNI) model has both ferromagnetic and antiferromagnetic interactions, competition plays an important role. In the three-dimensional ANNNI model, competing interactions lead to a rich phase diagram consisting of an infinite number of phases with periodicities ranging from single lattice sites to arbitrarily long repeat distances.[9] In two dimensions, the ANNNI Hamiltonian may be written as:

$$H = -\frac{1}{2} \sum_{i,j} J_0 S_{i,j} S_{i\pm 1, j\pm 1} + J_1 S_{i,j} S_{i\pm 2, j} \ , \qquad (1)$$

where $S_{i,j}$ is the spin orientation (± 1) on site i,j, and J_0 and J_1 are constants. The two-dimensional ANNNI phase diagram[10] for $J_0 > 0$ consists of a high-temperature paramagnetic phase, a low-temperature ferromagnetic phase for $J_1 < J_0/2$, a low-temperature ordered phase consisting of alternating stripes of two up and two down spins parallel to the j direction for $J_1 > J_0/2$, and an incommensurate phase between the striped and paramagnetic phases.

There have been several studies which suggest that ordering in the ANNNI model is more subtle than in the Ising model.[11,12] In a self-consistent mean-field study, Jensen and Bak[11] showed that the weakly interacting domain walls can be pinned to the lattice in essentially random sequences, which are metastable. Morgenstern[12] conducted a study of the ANNNI and the related brickwork ANNNI models, using both transfer matrix and Monte Carlo techniques. The Monte Carlo study was performed for long times (30 000 Monte Carlo steps per spin (MCS) on a narrow (64×8) lattice. He found that the domain walls never achieved their equilibrium positions, as determined by the transfer matrix calculation.

More recently, Monte Carlo simulations have been performed on the ANNNI model, using both nonconserved[13] (Glauber) and conserved[14] (Kawasaki) spin dynamics. In these simulations a two-dimensional ANNNI model was instantaneously quenched from $T \gg T_c$ to $T \ll T_c$. With nonconserved dynamics, $t^{1/2}$ growth of the correlation length was observed, with an anisotropic prefactor. Slowing was observed with Kawasaki dynamics, although it appears $t^{1/2}$ growth was observed asymptotically for long times. In work on a related model, Sadiq and Binder[15] performed a Monte Carlo quench study of an "isotropic" ANNNI model. For quenches to $T \simeq 0$, they observe extremely slow growth. However, since Kawasaki dynamics were employed, the relative importance of frustration is not clear.

In order to examine the effects of competing interactions on ordering kinetics and to resolve some of the confusion regarding ordering in the ANNNI model, we have performed a series of simulations in which a two-dimensional ANNNI model was quenched from $T \gg T_c$ to $T < T_c$ for a wide range of frustration parameters ($\kappa = -J_1/J_0$) and a number of temperatures. Nonconserved dynamics were chosen so that the role of frustration would be evident. In brief, we find that for $\kappa \leq 0$ the system rapidly forms domains which coarsen with $t^{1/2}$ kinetics. Similarly, for $\kappa \geq 1$ domains of striped phase form rapidly and coarsen with $t^{1/2}$ kinetics. However, for $0 < \kappa < 1$ quenches to low temperature result in the formation of a metastable glasslike phase which shows subpower law (logarithmic) growth. Quenches in this regime at higher temperatures lead to the slow formation of the ordered phase (i.e., the striped phase for $\kappa > \frac{1}{2}$ and the ferromagnetic phase for $\kappa < \frac{1}{2}$) and then domain growth with $t^{1/2}$ kinetics. A structure factor analysis is performed for the temporal and thermal evolution of the glasslike phase. Consequences of these results for the sensitivity of polytypic systems (i.e., systems with large numbers of nearly degenerate modulated phases, such as SiC) to preparation technique and history are discussed.

II. SIMULATION PROCEDURE

The present Monte Carlo simulations on the ANNNI model were performed on a square lattice. For the sake of later convenience we choose to normalize the ANNNI Hamiltonian [Eq. (1)] by the nearest-neighbor coupling constant J_0, such that the bond energy E_{ij} is

$$E_{ij} = -S_{ij}[S_{i+1,j} + S_{i-1,j} + S_{i,j+1} + S_{i,j-1} - \kappa(S_{i+2,j} + S_{i-2,j})]/2 , \quad (2)$$

where $\kappa = -J_1/J_0$. The temperature T has also been normalized by the nearest-neighbor coupling constant, J_0. The phase diagram for the two-dimensional ANNNI model is well established[10] and is indicated in Fig. 1. We shall denote the ferromagnetic phase by F, the paramagnetic phase by P, the incommensurate phase by I, and the modulated phase by $\langle 2 \rangle$, indicating that it corresponds to alternating stripes of two up and two down spins oriented perpendicular to the axial direction (i.e., the i direction).

In the present study, we perform Monte Carlo simulations of the evolution of the ANNNI model quenched from $T \gg T_c$ to a finite temperature $0.02 \leq T \leq 0.4$, for $-19.5 \leq \kappa \leq 20.0$. In addition, a series of simulations were performed at $T = 0.08$ by equilibrating the system in the ferromagnetic regime and discontinuously increasing κ to between 0.5 and 2.0. This results in a phase transformation from the small κ, F phase to the large κ, $\langle 2 \rangle$ phase. The simulations were performed with nonconserved dynamics and with a random updating scheme. The transition probability employed was

$$W = \tfrac{1}{2}[1 - \tanh(\delta E/2T)] , \quad (3)$$

where δE is minus the change in energy of the system due to an attempted spin flip [evaluated employing Eq. (2)]. All of the simulations were performed on 200×200 square lattices. The data presented below were averaged over five simulations (except for the nucleation and growth simulations where averaging would be inappropriate).

The simulations were analyzed by monitoring the magnitude of the structure factor in the axial (i) and perpendicular (j) directions every 100 MCS (1 MCS is defined as N spin flip attempts, where $N = 40\,000$ is the number of spins in the system). In addition, the energy of the system was measured every 20 MCS, and the spin configuration every 50 MCS. Previous simulations[16] indicate that the difference between the instantaneous energy of the system and that in its equilibrium state, ΔE, is inversely proportional to the correlation length in the system. The equilibrium energy was determined by putting the system in its $T = 0$ equilibrium configuration and then running for 2000 MCS at the temperature and κ value of interest.

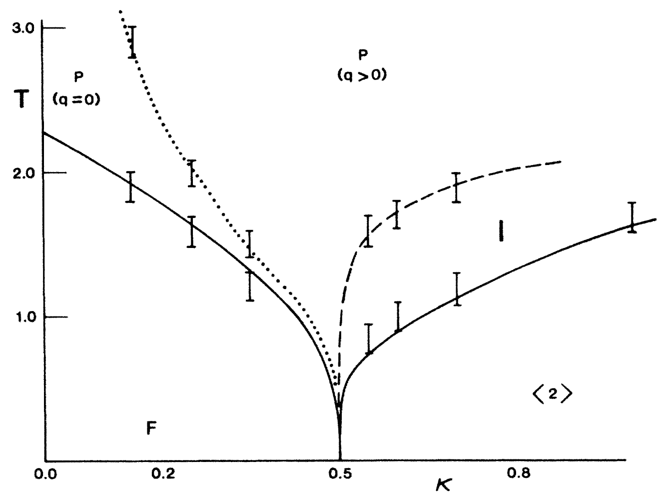

FIG. 1. The two-dimensional ANNNI phase diagram, after Beale, *et al.* (Ref. 10). F, $\langle 2 \rangle$, and I represent the ferromagnetic, striped, and incommensurate phases, respectively. The label P indicates the paramagnetic phase, which has a peak in $S(q=0)$ for small κ and a peak at $q > 0$ at larger κ, as indicated.

III. DOMAIN GROWTH FOLLOWING QUENCHES FROM THE PARAMAGNETIC STATE

A. $\kappa \leq 0$

The temporal evolution of the ANNNI microstructure following a quench from $T \gg T_c$ to $T = 0.02$ for

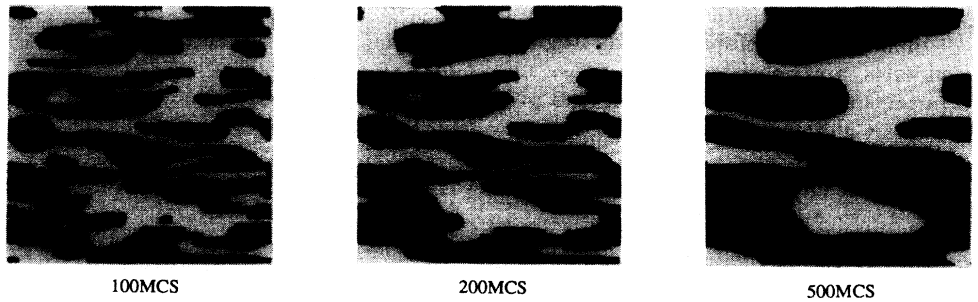

FIG. 2. The temporal evolution of the ANNNI microstructure following a quench from $T \gg T_c$ to $T = 0.02$ for $\kappa = -19.5$. The dark regions indicate areas of spin up and the light regions correspond to spin down.

$\kappa = -19.5$ is shown in Fig. 2. The microstructure produced is quite similar to that found in quenches of the usual Ising model. One pronounced difference which may be observed is the strong tendency for the domain walls to lie preferentially along the axial direction. This asymmetry may be traced to the relative energies of the domain walls parallel and perpendicular to the axial direction. Domain walls perpendicular to the axial direction have an energy of -2 per unit length. Those parallel to the axial direction have an energy of $-2(1-\kappa)$. Therefore, for $\kappa < 0$, domain walls lying in the axial direction are energetically preferred.

Further asymmetry may be seen by considering the structure factor parallel and perpendicular to the axial direction (see Fig. 3). The structure factor in both directions show peaks at $q \approx 0$. These peaks sharpen with time indicating the observed domain growth. However, comparison of the widths of the peaks in $S(q,0)$ with those in $S(0,q)$ indicates that the order is considerably more pronounced in the axial direction. This is consistent with the asymmetry in the direction along which the domain walls lie.

The time dependence of the correlation length is shown in Fig. 4 where we plot the energy deviation from the equilibrium state ΔE against time (ΔE is inversely proportional to the correlation length). Note that the curves corresponding to different values of κ are all parallel, indicating the κ independence of the growth exponent in this range of κ. Data from an Ising model ($\kappa = 0$) is also plotted on the curve for comparison. The measured

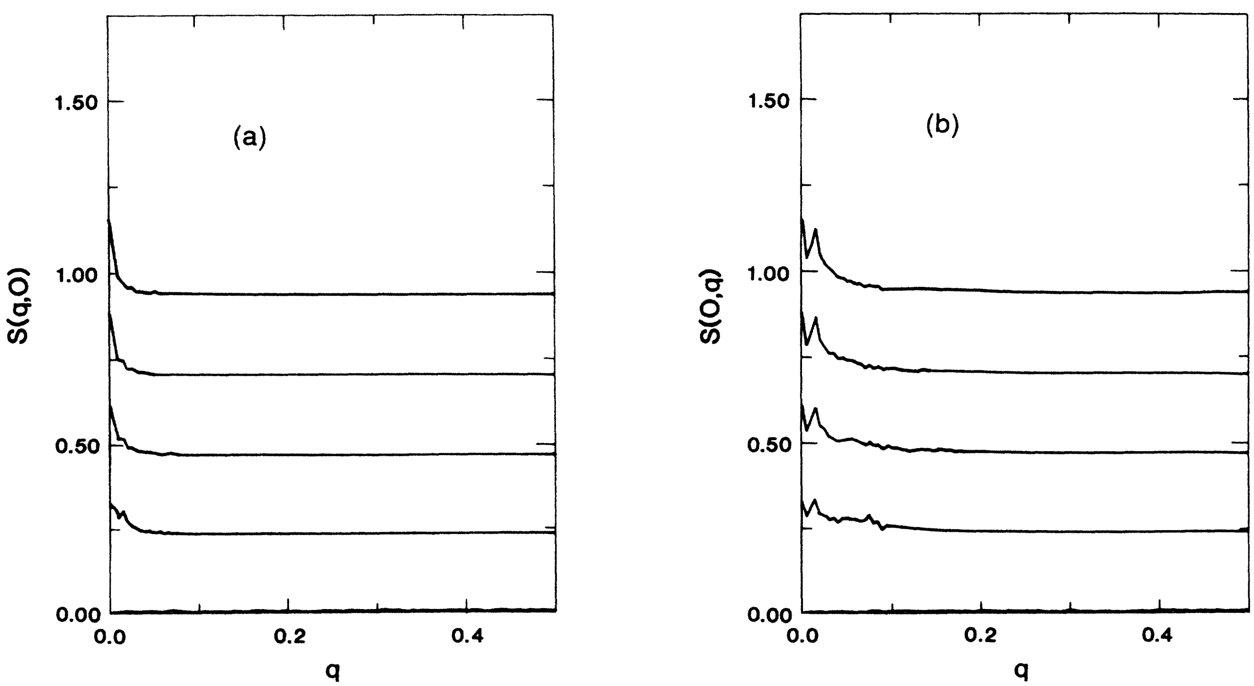

FIG. 3. The time dependence of the structure factor in the direction (a) parallel and (b) perpendicular to the axial (x) direction for the same conditions as in Fig. 2. The different curves in each figure correspond to 400, 300, 200, 100, and 0 MCS, in order from top to bottom. Arbitrary shifts were added to the structure factor for clarity.

slopes are consistent with the growth of the correlation length in a $t^{1/2}$ manner. Therefore, in this regime, domain growth kinetics are consistent with those observed in a wide variety of other spin systems[6,7] and predicted by Lifshitz,[4] and Cahn and Allen.[5]

B. $\kappa \geq 1$

For $\kappa \geq 1$, the next-nearest-neighbor antiferromagnetic interactions dominate the nearest-neighbor ferromagnetic interactions. The $\langle 2 \rangle$ state, which satisfies all of the antiferromagnetic interactions, is observed in Fig. 5 where a quench has been performed from $T \gg T_c$ to $T = 0.02$ at $\kappa = 20.0$. The $\langle 2 \rangle$ phase consists of alternating stripes of two up spins and two down spins oriented perpendicular to the axial (i) direction. Since the basic unit of the $\langle 2 \rangle$ phase consists of four spins, the model is clearly fourfold degenerate. The orientation of the domain walls in the $\langle 2 \rangle$ phase region depends on the relative energies of the domain walls. Since the model is fourfold degenerate, there are four types of domain walls in the $\langle 2 \rangle$ phase, as opposed to the one type of domain wall in the F phase. For $\kappa > 1$, the energies of the domain walls are such that the domain walls lying in the axial (i) direction are lower in energy than those in the perpendicular (j) direction. This asymmetry is manifested in the microstructures of Fig. 5 where clearly the domain walls lie preferentially in the axial (i) direction.

Figure 5 shows that the model has both three and fourfold vertices (i.e., three or four domain walls meet at a point), like the fourfold degenerate Potts and clock models, respectively. The fourfold vertices are generally such that as one circumscribes the vertex, the four-spin pattern of the $\langle 2 \rangle$ phase is phase shifted by one spin. This leads to two types of fourfold vertices having either a clockwise or counter-clockwise vorticity. Perhaps it is more appropriate to refer to the sense of the vertex in the framework of a Burgers vector (from dislocation theory) than vorticity since each fourfold vertex has associated with it an extra half-stripe either pointing up or down (corresponding to the extra half-plane of atoms above or below an edge dislocation with a Burgers vector pointing to the left or right). Threefold vertices may be thought of as partial dislocations separated by finite energy stacking faults.

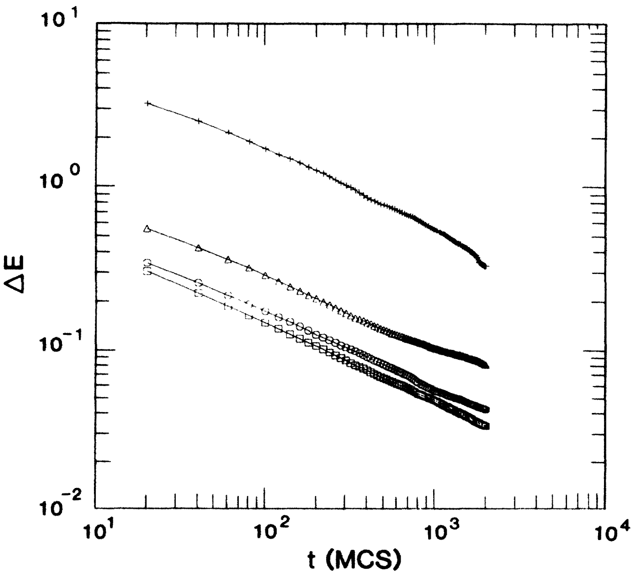

FIG. 4. The time dependence of the excess energy, ΔE, following a quench from $T \gg T_c$ to $T = 0.02$. The different curves correspond to $\kappa = 0$ (squares), -0.2 (circles), -1.5 (triangles), and -19.5 (+ 's).

The asymmetry between the axial and perpendicular directions may be seen in Fig. 6 where we show the time dependence of the structure factor in the axial and perpendicular directions. In the axial direction, a peak at $q = \frac{1}{4}$ forms at early times and sharpens with increasing time. The width of the peak indicates the $\langle 2 \rangle$-phase domain size. On the other hand, one should expect a peak at $q = 0$ in the structure factor in the perpendicular direction. However, the structure factor in the perpendicular direction is relatively flat and featureless. The lack of a pronounced peak may be traced to the preponderance of domain walls in the axial direction which tend to destroy long-range order in the perpendicular direction.

The temporal evolution of the correlation length (actually ΔE which is inversely proportional to the correlation length) is indicated in Fig. 7 for $1 \leq \kappa \leq 20$ at $T = 0.02$.

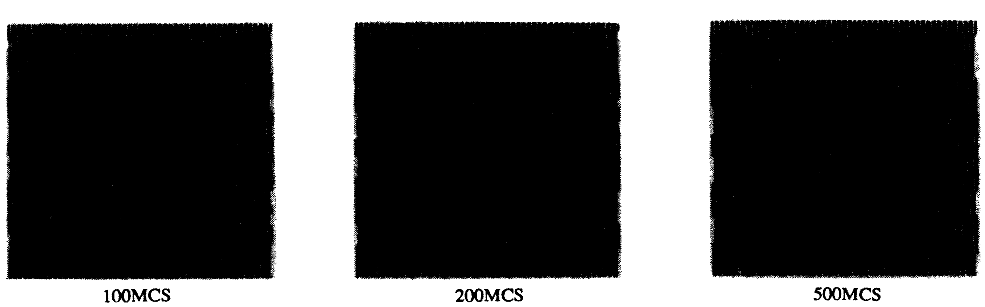

FIG. 5. The temporal evolution of the ANNNI microstructure following a quench from $T \gg T_c$ to $T = 0.02$ for $\kappa = 20.0$.

The slopes of these curves indicate that the correlation length is increasing as $t^{1/2}$ for all κ in this range. This result is consistent with that observed in the fourfold degenerate Potts and clock models. However, as pointed out by Kaski, *et al.*, the domain coarsening is anisotropic in that the growth in the axial and perpendicular directions occur at different rates. The effect of varying the temperature to which the model was quenched is indicated in Fig. 8 where the domain growth kinetics are plotted as a function of time. For times such that the correlation length in the system is small compared with the model size, the four data sets corresponding to $T=0.02$, 0.1, 0.2, 0.3, and 0.4 fall on the same curve. At late times, where the correlation length is of order the system size some deviation occurs, as expected. This result demonstrates that domain growth is insensitive to temperature for $T \ll T_c$.

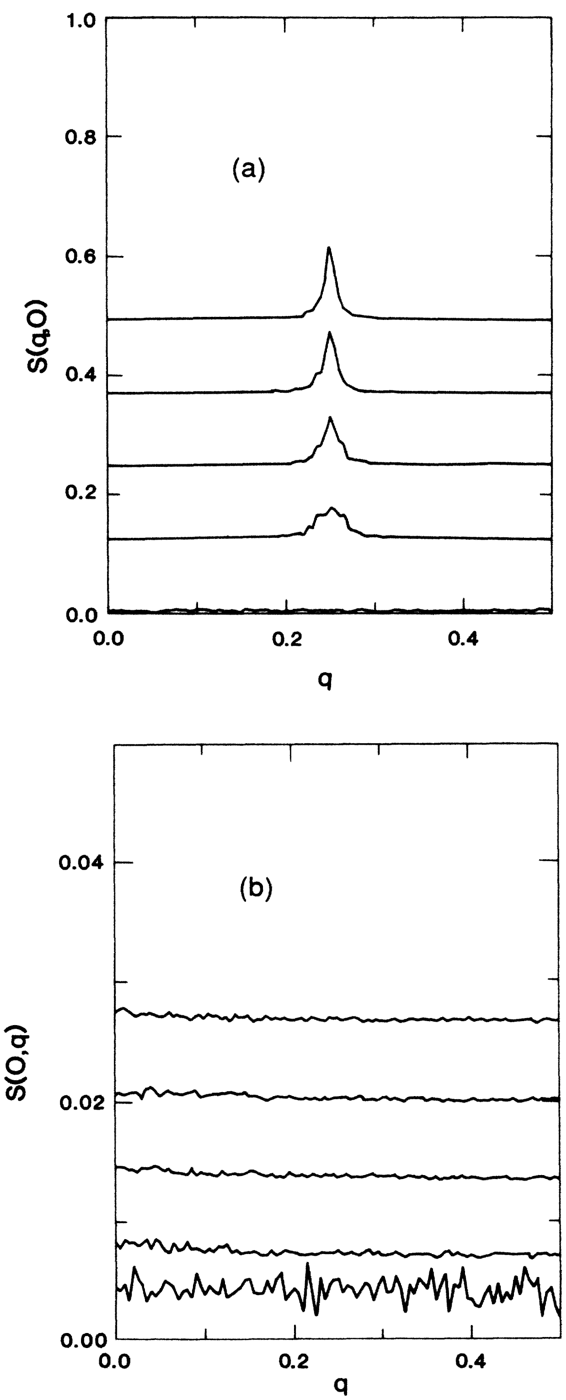

FIG. 6. The time dependence of the structure factor in the direction (a) parallel and (b) perpendicular to the axial (x) direction for the same conditions as in Fig. 5. The different curves in each figure correspond to 400, 300, 200, 100, and 0 MCS, in order from top to bottom.

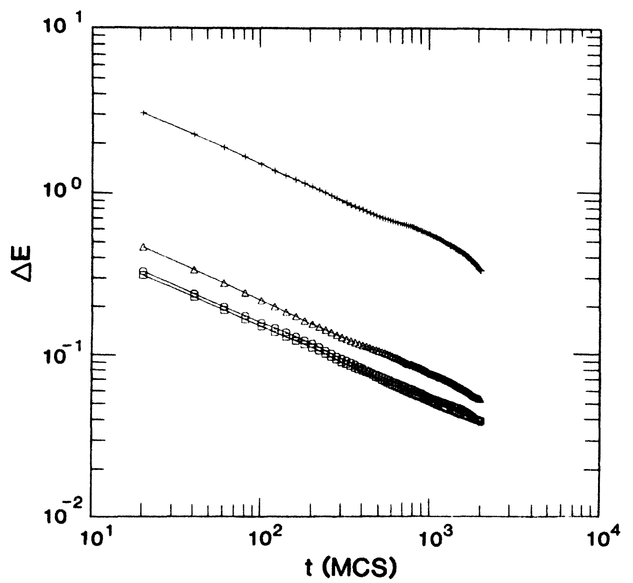

FIG. 7. The time dependence of the excess energy, ΔE, following a quench from $T \gg T_c$ to $T=0.02$. The different curves correspond to $\kappa=1$ (squares), 1.2 (circles), 2.0 (triangles), and 20.0 (+ 's).

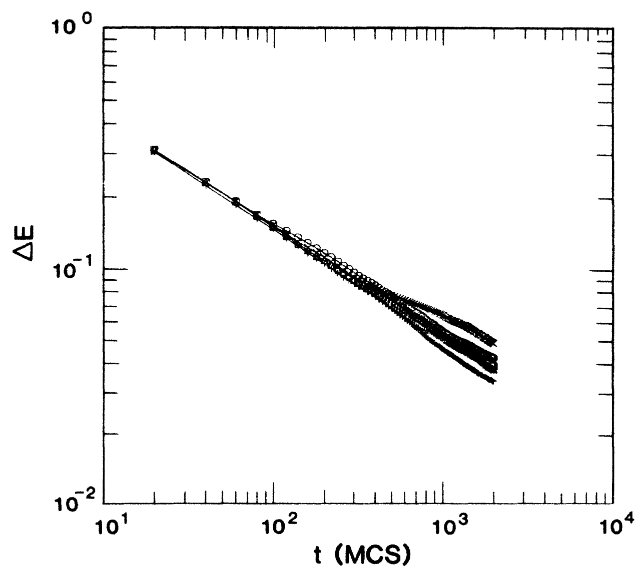

FIG. 8. The time dependence of the excess energy, ΔE, following a quench from $T \gg T_c$ to $T=0.02$ (squares), 0.1 (circles), 0.2 (triangles), 0.3 (+ 's), and 0.4 ($\times$'s) at $\kappa=1.0$.

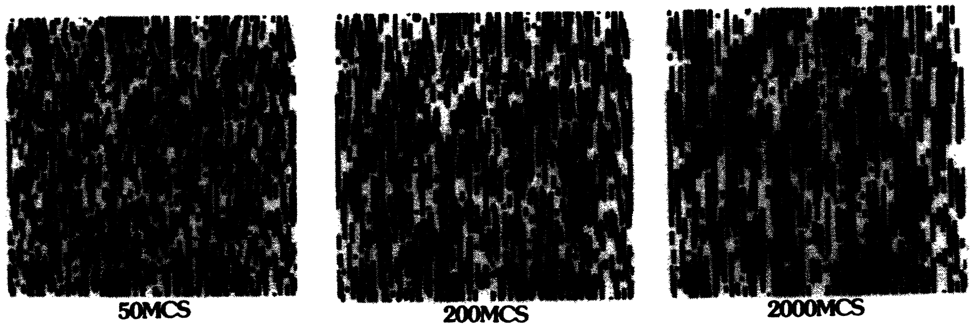

FIG. 9. The temporal evolution of the ANNNI microstructure following a quench from $T \gg T_c$ to $T = 0.02$ for $\kappa = 0.08$.

IV. AN ANNNI GLASS

A. $0 < \kappa < 1/2$

When the system is quenched from $T \gg T_c$ to $T \approx 0$ for $0 < \kappa < \frac{1}{2}$, microstructures such as those shown in Fig. 9 typically result. These microstructures appear disordered in that no clear F or $\langle 2 \rangle$ phase is visible. However, a crude striped morphology does form. These stripes, however are rather short and there is no significant correlation between neighboring stripes. In addition, the stripes vary in width from one spin to many spins. While these microstructures do appear to evolve in time, their evolution is very slow and they do not appear to be evolving toward their ferromagnetic ground state.

Structure factors measured as a function of time for quenches at $\kappa = 0.4$ and $T = 0.02$ are shown in Fig. 10. Clearly little temporal evolution is evident in the structure factors. The structure factors in the axial direction have near zero amplitude for $q > \frac{1}{4}$ and have some small, finite amplitude between $q = 0$ and $q = \frac{1}{4}$. A small peak is observed in the vicinity of $q = \frac{1}{4}$, as would be expected for the $\langle 2 \rangle$ phase. While this is consistent with the observed stripelike features in Fig. 9, it is surprising in that the equilibrium phase is ferromagnetic, which should yield a peak only at $q = 0$. In the perpendicular (j) direction, a peak forms at $q = 0$. However, this peak is of a much smaller amplitude than that seen where the ferromagnetic phase forms (see Fig. 3, above).

The temporal dependence of the correlation length for quenches in this regime of κ and $T = 0.02$ is indicated in Fig. 11. This plot clearly indicates that for $0 < \kappa < \frac{1}{2}$, the growth kinetics are subpower law. Figure 11 demonstrates that while the microstructure continues to evolve with time, it is doing so only very slowly.

These kinetics should be contrasted with those found

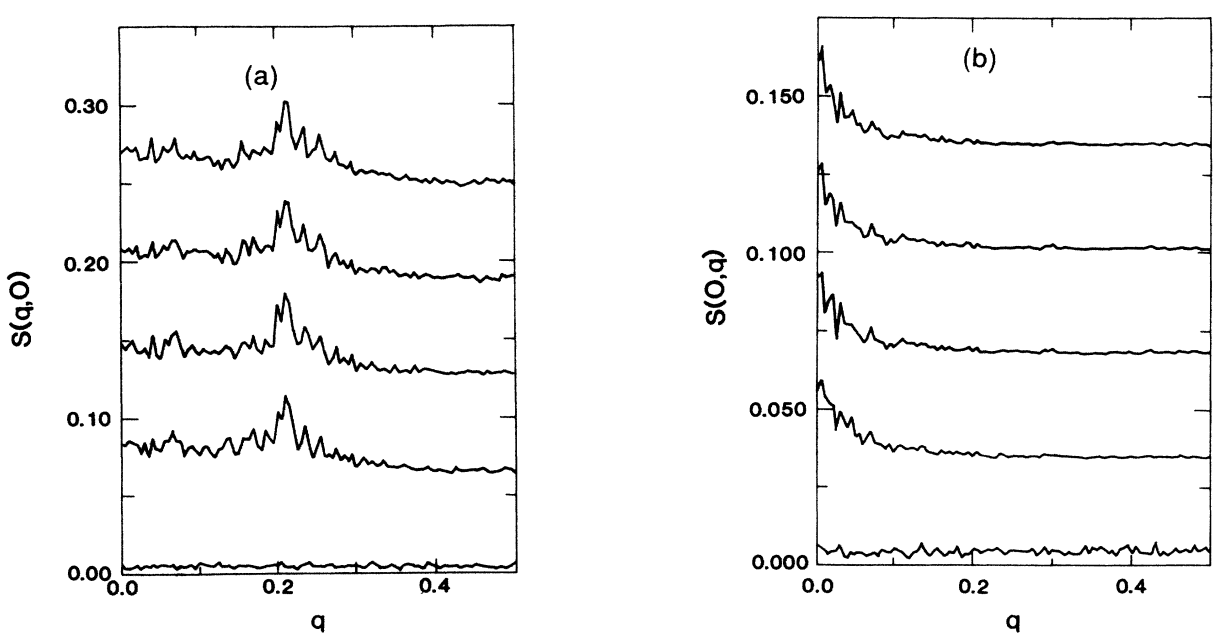

FIG. 10. The time dependence of the structure factor in the direction (a) parallel and (b) perpendicular to the axial (x) direction for a quench to $T = 0.02$ at $\kappa = 0.4$. The different curves in each figure correspond to 2000, 1500, 1000, and 500 MCS, in order from top to bottom.

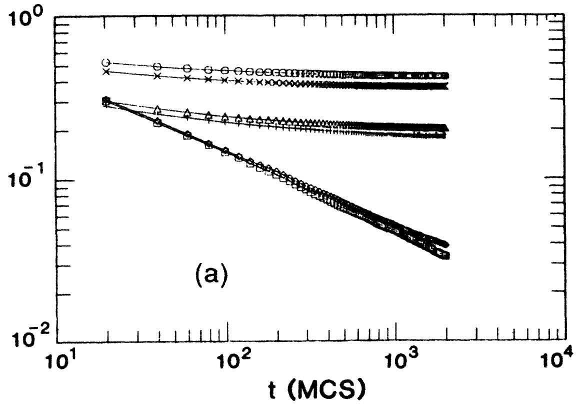

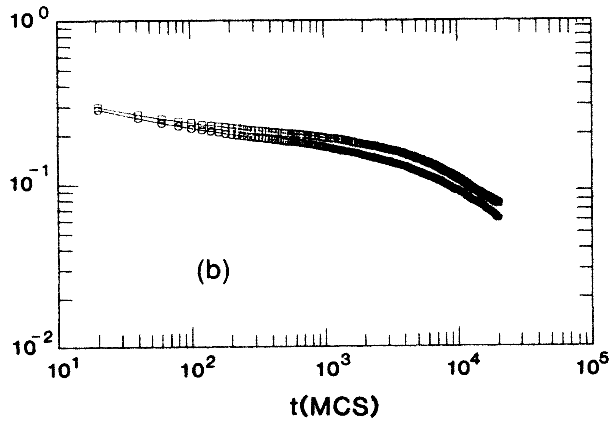

FIG. 11. The time dependence of the excess energy, ΔE, following a quench from $T \gg T_c$ to $T=0.02$. (a) The different curves correspond to $\kappa=0.2$ (circles), 0.8 ($\times$'s), 0.4 (triangles), 0.6 (+ 's), 1.0 (diamonds), and 0.0 (squares), in order from top to bottom. (b) Same as (a) but for runs out to 20 000 MCS. The upper curve is for $\kappa=0.4$ and the lower curve is for $\kappa=0.6$.

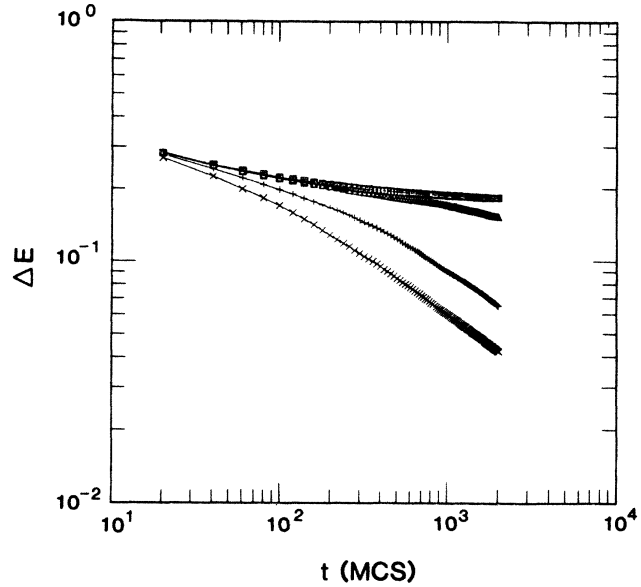

FIG. 12. The time dependence of the excess energy, ΔE, following a quench from $T \gg T_c$ to $T=0.02$ (squares), 0.1 (circles), 0.2 (triangles), 0.3 (+ 's), and 0.4 ($\times$'s) at $\kappa=0.4$.

following a quench to higher temperature within this same range of κ (still within the F phase field). Such a comparison is made in Fig. 12 for $\kappa=0.4$ and $T=0.02$, 0.1, 0.2, 0.3, and 0.4. This figure shows that there exists a temperature above which quenches yield power-law growth and below which yield logarithmic growth. For $\kappa=0.4$ this temperature is between 0.2 and 0.3 and for $\kappa=0.2$ this temperature is between 0.1 and 0.2. However, even for quenches below this critical or glass transition temperature, at sufficiently long times the kinetics asymptotically approach the normal $t^{1/2}$ behavior found for $\kappa \le 0$ [see Fig. 11(b)]. This type of behavior indicates that a glasslike phase will only be observed if the observation time is short compared with the ordering time. The rather slow transition from logarithmic growth to power-law growth indicates that the change is more a thermally activated, continuous ordering phenomena than a nucleation and growth phenomena.

The temperature dependence of the final (2000 MCS following the quench) microstructures is indicated in Fig. 13. Both the structure factors parallel and perpendicular to the axial direction show pronounced differences between $T=0.2$ and $T=0.3$. This supports the kinetic information that there is a transition from the glasslike phase to the ferromagnetic phase in this temperature range. The transition between these two phases is indicated in Fig. 14 where the structure factor for $\kappa=0.4$ and $T=0.3$ shows a slow, continuous increase in peak height at $q=0$ with increasing time. This result confirms the idea that the transition from the glasslike phase to the ferromagnetic phase is continuous.

B. $1/2<\kappa<1$

In Fig. 15 we show a series of spin configurations corresponding to different times following a quench from $T \gg T_c$ to $T=0.08$, for $\kappa=0.8$. Microstructures essentially indistinguishable from these occur on low temperature quenches in the entire $\langle 2 \rangle$-phase field for $\frac{1}{2}<\kappa<1$. Although this temperature and κ are well within the ordered $\langle 2 \rangle$-phase region of the phase diagram (Fig. 1), the characteristic two spin wide stripe pattern clearly does not form. Instead we observe a disordered phase which does not appear to be evolving toward the equilibrium $\langle 2 \rangle$ state. Comparison of the spin configurations at early times (e.g., 200 MCS) and late time (e.g., 2000 MCS) shows little difference. There does, however, appear to be an extremely slow increase in the correlation length with time. Although the equilibrium $\langle 2 \rangle$ phase does not appear, short-range order clearly exists. The presence of short-range order with no accompanying long-range order is a common feature of glassy systems. The microstructures quenched into this region of the phase diagram are nearly indistinguishable from those quenched to low temperature for $0<\kappa<\frac{1}{2}$, where the equilibrium state is ferromagnetic.

The time dependence of the structure factor for a quench from $T \gg T_c$ to $T=0.02$ at $\kappa=0.6$ is shown in Fig. 16. As in the case of a low-temperature quench for $0<\kappa<\frac{1}{2}$, the structure factor in the axial direction show only a very small amplitude for $q>\frac{1}{4}$ and a larger amplitude in the range $0<q<\frac{1}{4}$. While the amplitude is largest around $q=\frac{1}{4}$ (indicative of the $\langle 2 \rangle$ state), it is interesting to note that an increased amplitude is also present in the vicinity of $q=0$ (although not at exactly $q=0$). This result shows the remarkably strong competition between the ferromagnetic state and $\langle 2 \rangle$ phase, even

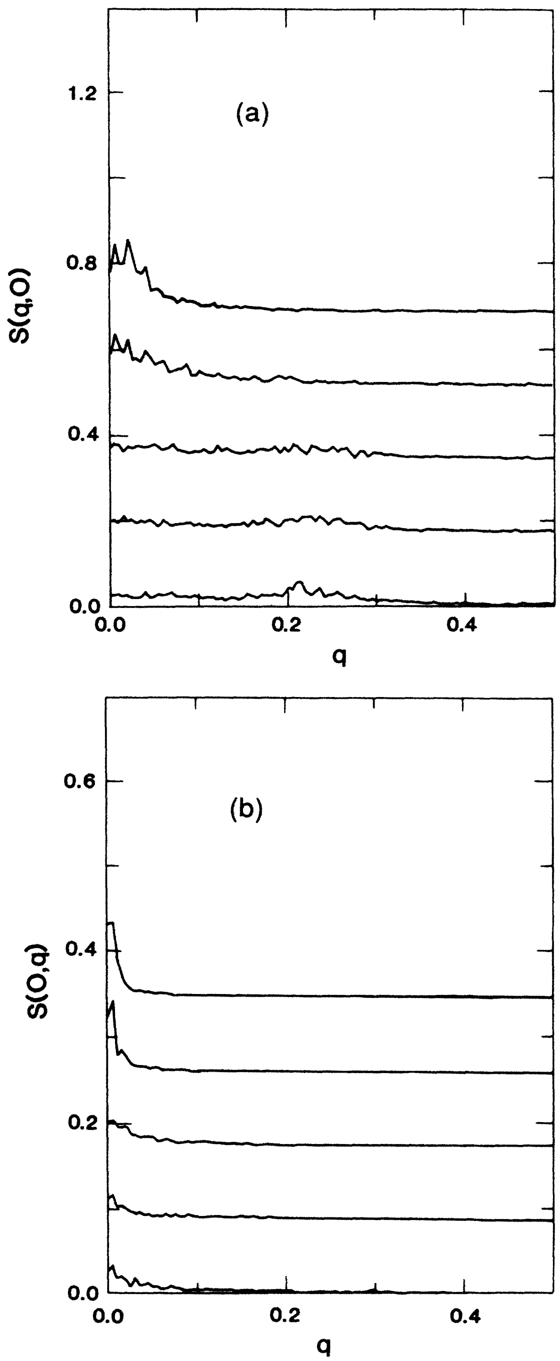

FIG. 13. The temperature dependence of the structure factor in the direction (a) parallel and (b) perpendicular to the axial (x) direction 2000 MCS following the quench at $\kappa=0.4$. The different curves in each figure correspond to quench temperatures of 0.4, 0.3, 0.2, 0.1, and 0.02, in order from top to bottom.

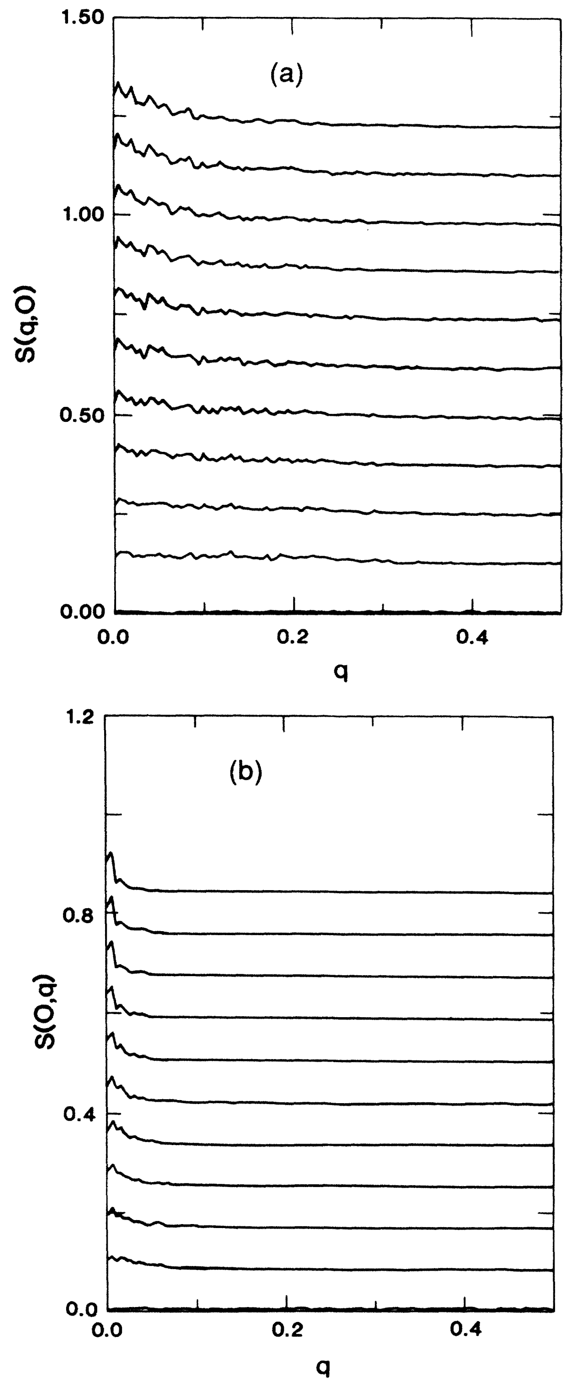

FIG. 14. The time dependence of the structure factor in the direction (a) parallel and (b) perpendicular to the axial (x) direction for a quench from $T \gg T_c$ to $T=0.3$ at $\kappa=0.4$. The different curves correspond to times decrementing by 200 MCS from the top curve (2000 MCS) down.

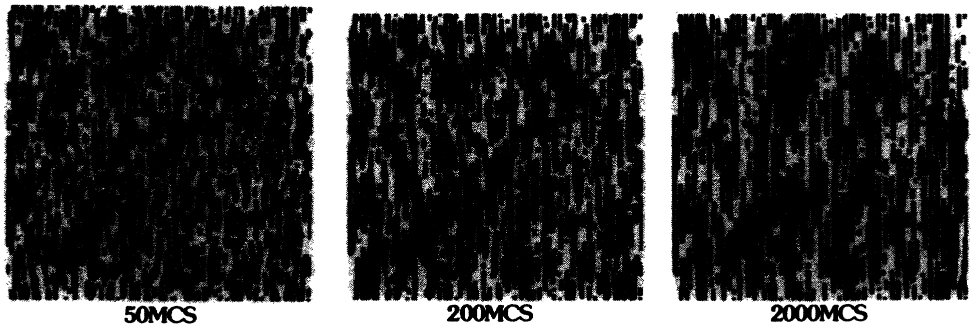

FIG. 15. The temporal evolution of the ANNNI microstructure following a quench from $T \gg T_c$ to $T = 0.02$ for $\kappa = 0.08$.

when κ is well within the $\langle 2 \rangle$-state phase field. In the perpendicular (j) direction, the model clearly has ferromagnetic tendencies, as indicated by the peak around $q = 0$. The $q = 0$ peak in this direction is indicative of both ferromagnetic and $\langle 2 \rangle$ ordering. The amplitude of this peak appear to be slowly increasing with time, although no clear $\langle 2 \rangle$ or ferromagnetic ordering is apparent in the microstructures.

The temporal dependence of for quenches to $T = 0.02$ for $\frac{1}{2} < \kappa < 1$ is indicated in Fig. 11. In the range of κ between $\frac{1}{2}$ and 1, the growth is subpower law, indicative of a kinetically frozen system. As with the microstructures and structure factors, the growth kinetics appear to evolve in a manner indistinguishable from those of systems quenched into the low temperature, ferromagnetic region of κ space ($0 < \kappa < \frac{1}{2}$). The parallels are particularly striking when comparing the $\kappa = 0.4$ and 0.6 quenches and the $\kappa = 0.2$ and 0.8 quenches, which are equally far from the transition at $\kappa = \frac{1}{2}$ but in completely distinct phase fields.

Just as with the low-temperature quenches into the $0 < \kappa < \frac{1}{2}$ ferromagnetic phase field, increasing the temperature to which the quench was performed leads to the formation of the equilibrium phase for $\frac{1}{2} < \kappa < 1$ (see Fig. 17). For $T > 0.2$ at $\kappa = 0.6$ and for $T > 0.1$ at $\kappa = 0.8$, the $\langle 2 \rangle$ state appears to form and exhibits power law kinetics within the 20000 MCS simulations. However, the $\langle 2 \rangle$ state does appear even at lower temperatures given sufficient time [see Fig. 11(b)]. As for all true glasses, the glass transition temperature is only defined once the time scale of observation is set. The existence of a transition temperature is also seen by consideration of the structure factor after the 2000 MCS "equilibration" following the quench for systems quenched to different temperatures at $\kappa = 0.6$ (Fig. 18). As indicated by the temporal dependence of the correlation length, a real transition is observed for $T > 0.2$ at this value of κ. However, hints of the impending transition from the glasslike phase to the equilibrium $\langle 2 \rangle$ phase may already be seen at $T = 0.2$. It is interesting to note that the transition from the glassy phase to the $\langle 2 \rangle$ phase is accompanied by the expected increase in the $q = \frac{1}{4}$ correlation in the axial direction, but a pronounced *decrease* in the $q = 0$ correlation in the perpendicular (j) direction. This unexpected feature must be attributed to the formation of domain walls which shift the stripes out of registry.

V. QUENCHES FROM THE FERROMAGNETIC TO $\langle 2 \rangle$ PHASE

While in the previous sections we have considered rapid changes in temperature from $T \gg T_c$ to $T < T_c$ at constant κ, in the present section we consider rapid changes in κ from well within the ferromagnetic state to well within the $\langle 2 \rangle$-phase field at constant temperature. Such studies are useful since in most real materials changes in temperature are accompanied by changes in the strength of the interaction parameter. These simulations were all performed for quenches at $T = 0.08$. We find that for quenches (in κ, not T) from the equilibrium ferromagnetic phase to $\kappa \geq 2$, the $\langle 2 \rangle$ phase forms rapidly and a coarsening $\langle 2 \rangle$-phase domain structure is observed (see Fig. 19). The resultant microstructures are essentially indistinguishable from those observed in temperature quenches from $T \gg T_c$ to $T \ll T_c$ for $\kappa \geq 1$. Similarly, the evolution of the correlation length following κ quenches in this range yield the same $t^{1/2}$ kinetics as in the thermal quenches for $\kappa \geq 1$.

While κ quenches at $T = 0.08$ for $\kappa \geq 2$ led to the immediate formation of the $\langle 2 \rangle$ phase, quenches to $1.6 < \kappa < 2$ led to the formation of the $\langle 2 \rangle$ phase by classical nucleation and growth. The temporal evolution of the spin configuration following a quench to $\kappa = 1.7$ at $T = 0.08$ is shown in Fig. 20. Under these conditions the spin configuration remains entirely ferromagnetically ordered for the first approximately 100 MCS, following which a single spin flip is thermally activated. The single spin nucleates a stripe which grows. Additional stripes are nucleated either homogeneously or heterogeneously and growth proceeds until the system is essentially all $\langle 2 \rangle$ phase with domain walls. Due to the rapid formation of the $\langle 2 \rangle$ phase along the stripes relative to the slow advance in the axial direction, the domain walls in this system appear preferentially oriented parallel to the stripes. Although the orientation of these domain walls contradicts the argument given above for the preferred domain wall orientation following thermal quenches, this orientation preference is dictated by kinetic rather than energetic constraints.

For $\kappa > 1$, the spins adjacent to this first spin to flip, can flip with no energy cost, and the stripe can grow. Once a single stripe is growing, additional stripes form in any one of three ways. First, the growing stripe can locally become wider than its nominal two-spin width. This locally "two wide" stripe can then split and form two parallel stripes. Second, new stripes can be formed by thermally activated flipping of a spin remote from the initial stripe. Finally, a growing stripe can grow through the periodic boundary conditions and, if not perfectly aligned with its own other end, it appears as a new stripe. Although this results in some unwanted correlation between stripes due to the finite system size, this mechanism is not entirely unphysical as it can be viewed as a consequence of nucleation in an adjacent subcell of the mock-infinite system. In this sense, we can view mechanism 3 as indistinguishable from mechanism 2. In a number of test runs in which the stripe was nucleated we observed all three mechanism operating.

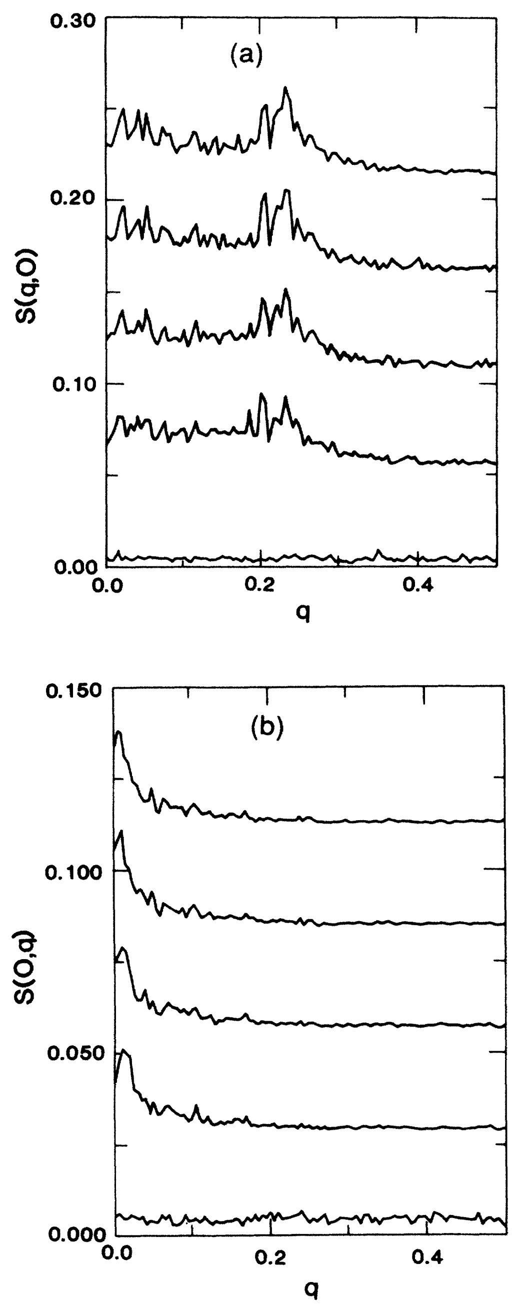

FIG. 16. The time dependence of the structure factor in the direction (a) parallel and (b) perpendicular to the axial (x) direction for a quench to $T=0.02$ at $\kappa=0.6$. The different curves in each figure correspond to 2000, 1500, 1000, and 500 MCS, in order from top to bottom.

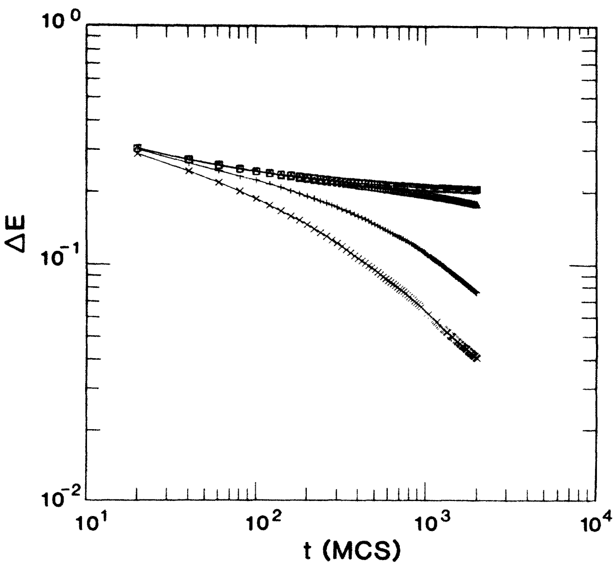

FIG. 17. The time dependence of the excess energy, ΔE, following a quench from $T \gg T_c$ to $T=0.02$ (squares), 0.1 (circles), 0.2 (triangles), 0.3 (+ 's), and 0.4 ($\times$'s) at $\kappa=0.6$.

The temporal evolution of the energy of the system following a κ quench to $\kappa=1.7$, 1.8, 1.9, and 2.0 at $T=0.08$ is plotted in Fig. 21. The incubation time, corresponding to the time waited for nucleation, is of order 100 MCS for the $\kappa=1.7$ simulation and is clearly greater than zero for $\kappa=1.8$. Following nucleation and transient growth, the system always exhibit the typical $t^{1/2}$ type growth kinetics. The statistics are considerably worse in this plot then in previous plots due to the fact that no averaging of the data was performed such that the effects of individual nucleation and growth events could be observed.

VI. DISCUSSION

While the phases observed following the quenches do not necessarily agree with the known equilibrium phase diagram, simple energetic/growth arguments are often sufficient to identify the bounds on the kinetically limited phases. The most important kinetic phase boundary to try to understand is that separating the glassy phase from the equilibrium phase.

Consider the case of the growth of a single stripe for $\kappa > \frac{1}{2}$. For an individual stripe to grow in the perpendicular (j) direction, its tip must be able to advance through all possible environments presented by the quench from high temperature. The most unfavorable configuration that the tip must be able to surpass occurs when, say, the up-spin stripe encounters a region of down spins at its tip. This is equivalent to the growth of a stripe of up spins into a system of otherwise down spins. Application of Eq. (2) to this geometry shows that the energy required

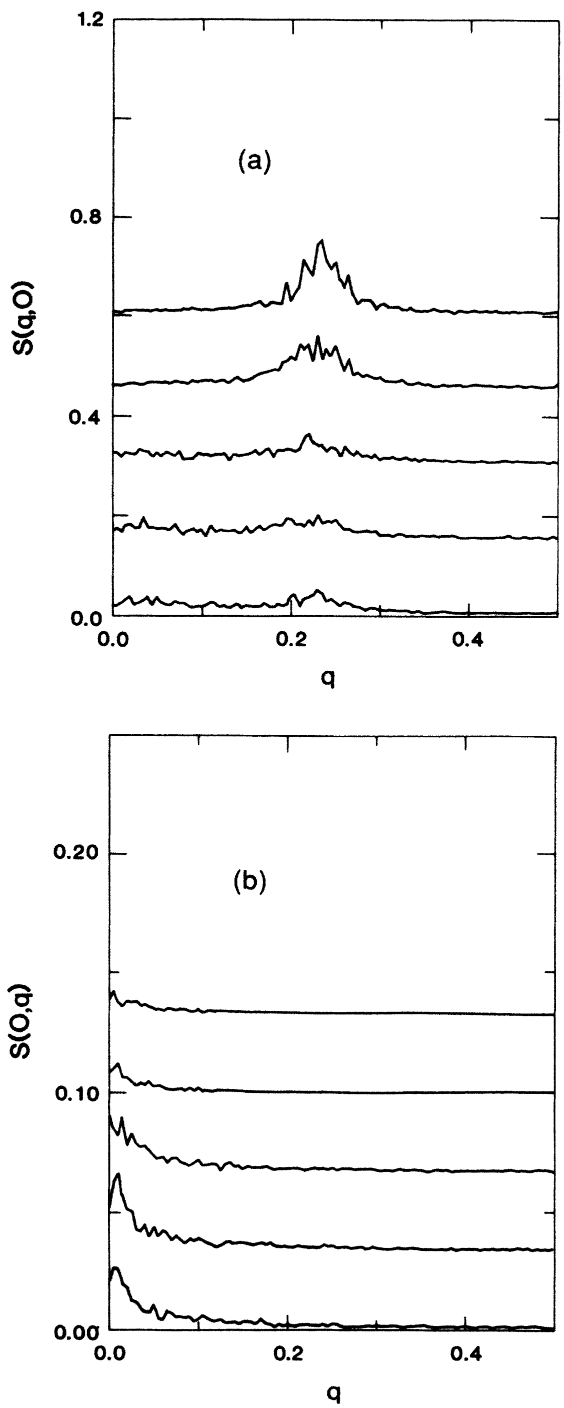

FIG. 18. The temperature dependence of the structure factor in the direction (a) parallel and (b) perpendicular to the axial (x) direction 2000 MCS following the quench at $\kappa=0.6$. The different curves in each figure correspond to quench temperatures of 0.4, 0.3, 0.2, 0.1, and 0.02, in order from top to bottom.

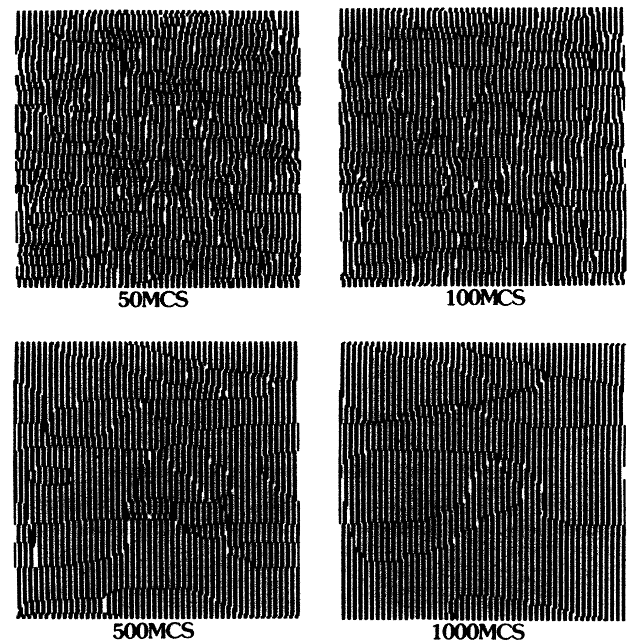

FIG. 19. The temporal evolution of the ANNNI microstructure at $T=0.08$ and $\kappa=2.0$, where the spin configuration was ferromagnetically ordered at 0 MCS

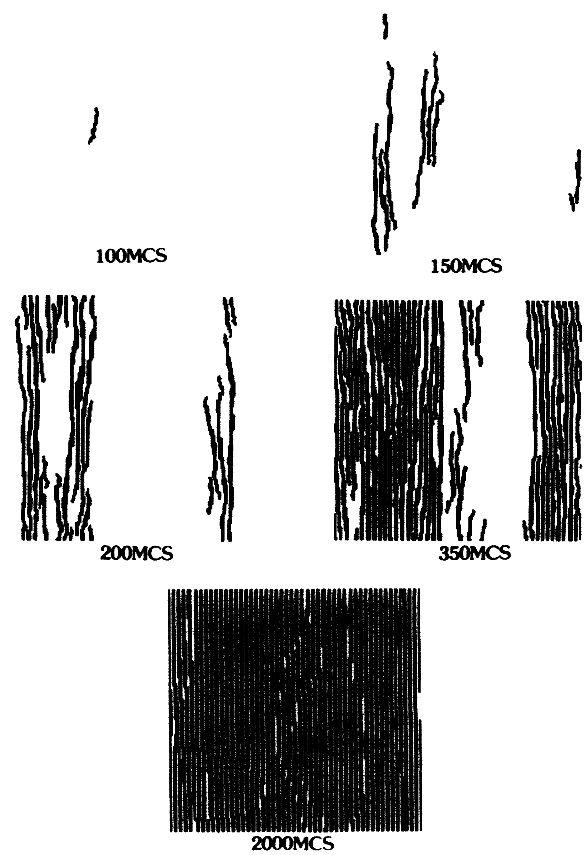

FIG. 20. The temporal evolution of the ANNNI microstructure at $T=0.08$ and $\kappa=1.7$, where the spin configuration was ferromagnetically ordered at 0 MCS.

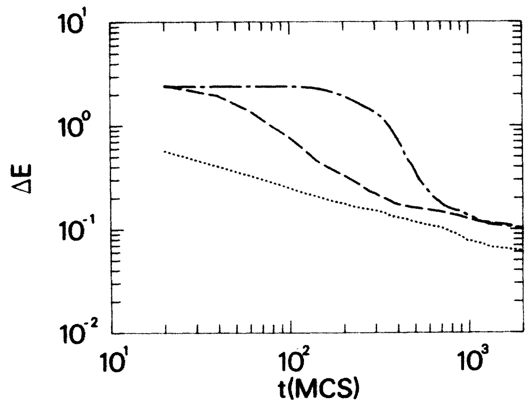

FIG. 21. The time dependence of the excess energy, ΔE, at $T=0.08$, where the spin configuration was ferromagnetically ordered at 0 MCS. The different curves correspond to $\kappa=1.7$ (chain dash), 1.8 (chain dot), 1.9 (dash), and 2.0 (dot), respectively. Note, these curves represent data from only one simulation each.

for this type of growth is proportional to $1-\kappa$. Therefore, only for $\kappa>1$ can the $\langle 2 \rangle$ phase form following a quench to $T=0$. For $\frac{1}{2}<\kappa<1$, the $\langle 2 \rangle$ phase can form only by thermally activated growth. The required thermal activation increases with decreasing κ. This argument reproduces the simulation results that the $\langle 2 \rangle$ phase forms spontaneously only for $\kappa \geq 1$ and that the apparent glass transition temperature increases with decreasing κ.

For quenches from high T to low T for $\kappa<\frac{1}{2}$, the critical configuration is the shrinking or decay of a single stripe. Application of Eq. (2) to this configuration, shows that the energy required to shrink such a stripe is proportional to κ. Therefore, for $\kappa \leq 0$ the ferromagnetic phase can form spontaneously, in agreement with the simulation results. However, for $0<\kappa<\frac{1}{2}$ the ferromagnetic phase must form by activated growth and hence will not form on quenches to $T=0$. Since the energy required to form the ferromagnetic phase scales with κ, the glass transition temperature should increase with increasing κ in this regime of κ.

This simple analysis suggests that the glass transition temperature in the equilibrium ferromagnetic region of the phase diagram should decay linearly with the magnitude of the frustration parameter, κ. Similarly, in the equilibrium $\langle 2 \rangle$-phase field, the glass transition temperature should scale linearly with $1-\kappa$. The magnitude of the transition temperature also depends on the length of the observation or, equivalently, on how long we are willing to run the simulation. Recognizing that the time required for the formation of the equilibrium phase scales as the exponential of the energy barrier over the temperature, we expect the glass transition temperature to scale inversely with the logarithm of the observation time. This relative insensitivity of the transition temperature to the duration of the observation is another hallmark of a glass. The linear dependence of the glass transition temperature on κ in the ferromagnetic regime and on $1-\kappa$ in the $\langle 2 \rangle$ regime suggests that in the vicinity of the multicritical point ($\kappa=\frac{1}{2}$), the equilibrium phase will never be achieved for any observation time. However, very close to the phase lines critical effects may become important.

For κ quenches at constant temperature, we found that for $\kappa \geq 2$, the initially ferromagnetic phase destabilizes and the $\langle 2 \rangle$ phase is formed immediately. Further, our simulations have shown that the $\langle 2 \rangle$ phase forms by nucleation and growth for systems quenched to $1.6<\kappa<2.0$ at $T=0.08$. Both of these phenomena can be understood in terms of the same type of energetic/growth arguments employed above. Consider first the energy required to flip the first spin in a ferromagnetically ordered system. The energy required for such a spin flip is proportional to $2-\kappa$. Once this first spin flips, the energy required to continue growing the stripe is proportional to $1-\kappa$, as discussed above. Therefore, for $\kappa \geq 1$ the critical nucleus is a single spin. This then suggests that there is no barrier for growth at $\kappa \geq 1$. Further, even if such a spin manages to form for $\kappa<1$, it will not grow. In other words, the critical nucleus for $\kappa<1$ is of infinite extent. For $1 \leq \kappa<2$, the nucleation event occurs via a thermal activation of an individual spin flip. Setting the nucleation time equal to the exponential of the activation energy over the temperature (0.08 in these simulations), we find typical nucleation times of order 12 000 MCS for $\kappa=1.6$, 75 MCS for $\kappa=1.7$, 0.5 MCS for $\kappa=1.8$, and 0.003 MCS for $\kappa=1.9$. These crudely estimated nucleation times are in good agreement with the simulation results (see Fig. 18).

In as much as ANNNI or ANNNI-like models are employed as models of phase behavior of real materials, the present simulations provide kinetic results which should be incorporated in interpreting observed phases. It has recently been suggested[17] that the application of this type of model can explain polytypism (the arrangement of identical or nearly identical structural units to create an ordered structure) in a wide class of materials. The prototypical polytypic system is SiC in which the stacking sequence of the close packed planes repeats periodically. More than 100 different stacking sequences are known. Polytypes of SiC are known to have repeat distances varying between 0.5048 and 1200 nm.[18]

The stacking sequences observed are known to depend sensitively on the method and conditions of preparation of the sample. Strong sensitivity to the details of the conditions under which the material was prepared is generally a signature of the presence of metastability. The large range of observed crystal structures in SiC suggests that there are a large number of nearly degenerate states very close in energy to the true ground state. However, even if a large number of different equilibrium states exist, the present simulations suggest that some of the observed crystal structures may be determined more by kinetic frustration than equilibrium considerations. The present simulations further suggest that it may be possible to form essentially random stacking sequences in polytype prone materials such as SiC under severe deposition conditions. Experimental work by Shinozaki and Sato[19] provides evidence that such random stackings do indeed occur.

VII. SUMMARY

A large number of Monte Carlo simulations of ordering in the two-dimensional ANNNI following a quench have been performed on large lattices using nonconserved dynamics for a wide range of frustration parameters, κ, and temperatures. It was found that in quenches from $T \gg T_c$ to $T < T_c$ for $\kappa \leq 0$ (i.e., in the ferromagnetic regime) ordered domains form quickly and coarsen with the expected $t^{1/2}$ kinetics. Similarly, quenches from $T \gg T_c$ to $T < T_c$ for $\kappa \geq 1$ (i.e., in the striped, $\langle 2 \rangle$-phase regime) quickly produce striped domains which also coarsen with the expected $t^{1/2}$ kinetics. However, for $0 < \kappa < 1$, quenches to low temperature produce a disordered, "glassy" phase, which shows logarithmic ordering kinetics and is insensitive to whether the underlying ground state is ferromagnetic or $\langle 2 \rangle$ phase. Quenches to higher temperatures show the presence of a finite glass transition temperature. Discontinuous changes in the value of the frustration parameter from the ferromagnetic to $\langle 2 \rangle$-phase region of the phase diagram at low temperature yields a phase change which occurs via classical nucleation and growth. A simple energetic/growth model has been proposed which accounts for all of the temperatures at which the ordering kinetics undergo transitions.

[1]J. D. Gunton, M. San Miguel, and P. S. Sahni, in *Phase Transitions and Critical Phenomena,* edited by C. Domb and J. L. Lebowitz (Academic, New York, 1983), Vol. 8, p. 267.

[2]P. S. Sahni, G. S. Grest, M. P. Anderson, and D. J. Srolovitz, Phys. Rev. Lett. **50**, 263 (1983); P. S. Sahni, D. J. Srolovitz, G. S. Grest, M. P. Anderson, and S. A. Safran, Phys. Rev. B **28**, 2705 (1983).

[3]K. Kaski, J. Nieminem, and J. D. Gunton, Phys. Rev. B **31**, 2998 (1985).

[4]I. M. Lifshitz, Zh. Eksp. Teor. Fiz. **42**, 1354 (1962) [Sov. Phys.—JETP **15**, 939 (1962)].

[5]S. M. Allen and J. W. Cahn, Acta Metall. **27**, 1085 (1979).

[6]P. S. Sahni, G. S. Grest, and S. A. Safran, Phys. Rev. Lett. **50**, 60 (1983); S. A. Safran, P. S. Sahni, and G. S. Grest, Phys. Rev. B **28**, 2693 (1983).

[7]M. K. Phani, J. L. Lebowitz, M. H. Kalos, and O. Penrose, Phys. Rev. Lett. **45**, 366 (1980); P. S. Sahni, G. Dee, J. D. Gunton, M. K. Phani, J. L. Lebowitz, and M. H. Kalos, Phys. Rev. B **24**, 410 (1981); E. T. Gawlinski, M. Grant, J. D. Gunton, and K. Kaski, Phys. Rev. B **31**, 281 (1985).

[8]I. M. Lifshitz and V. V. Slyozov, J. Phys. Chem. Solids **19**, 35 (1961).

[9]P. Bak and J. von Boehm, Phys. Rev. B **21**, 5297 (1980); J. von Boehm and P. Bak, Phys. Rev. Lett. **42**, 122 (1979).

[10]J. Villain and P. Bak, J. Phys. (Paris) **42**, 657 (1981); P. Beale, P. M. Duxbury, and J. Yeomans, Phys. Rev. B **31**, 7166 (1985).

[11]M. H. Jensen and P. Bak, Phys. Rev. B **29**, 6280 (1984).

[12]I. Morgenstern, Phys. Rev. B **29**, 1458 (1984).

[13]K. Kaski, T. Ala-Nissila, and J. D. Gunton, Phys. Rev. B **31**, 310 (1985).

[14]T. Ala-Nissila, J. D. Gunton, and K. Kaski, Phys. Rev. B **33**, 7583 (1986).

[15]A. Sadiq and K. Binder, J. Stat. Phys. **35**, 517 (1984).

[16]J. Vinals, M. Grant, M. San Miguel, J. D. Gunton, and E. T. Gawlinski, Phys. Rev. Lett. **54**, 1264 (1985); G. S. Grest and D. J. Srolovitz, Phys. Rev. B **32**, 3014 (1985).

[17]J. Smith, J. Yeomans, and V. Heine, in *Modulated Structure Materials,* edited by T. Tsakalakos (Martinus Nijhoff, Dordrecht, 1984), p. 95; G. D. Price and J. Yeomans, Acta Cryst. B **40**, 448 (1984).

[18]G. C. Trigunayat and G. K. Chadha, Phys. Status Solidi A **4**, 9 (1971).

[19]S. S. Shinozaki and H. Sato, J. Am. Ceram. Soc. **61**, 425 (1978).

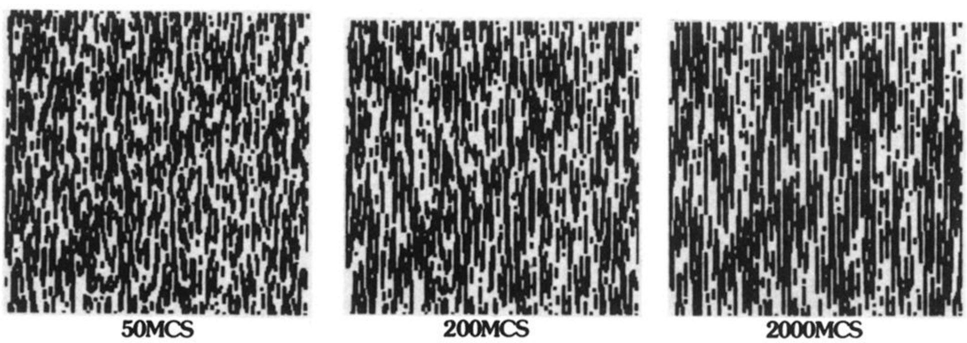

FIG. 15. The temporal evolution of the ANNNI microstructure following a quench from $T \gg T_c$ to $T=0.02$ for $\kappa=0.08$.

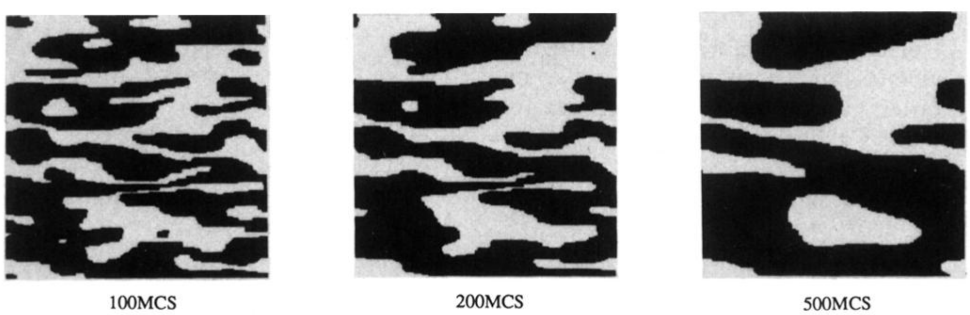

FIG. 2. The temporal evolution of the ANNNI microstructure following a quench from $T \gg T_c$ to $T = 0.02$ for $\kappa = -19.5$. The dark regions indicate areas of spin up and the light regions correspond to spin down.

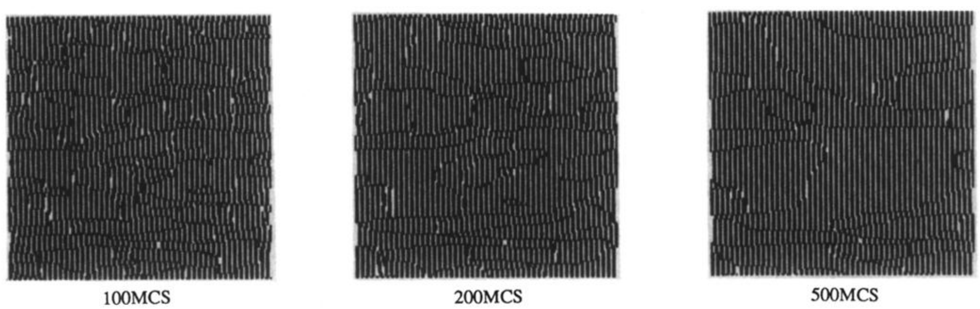

FIG. 5. The temporal evolution of the ANNNI microstructure following a quench from $T \gg T_c$ to $T=0.02$ for $\kappa=20.0$.

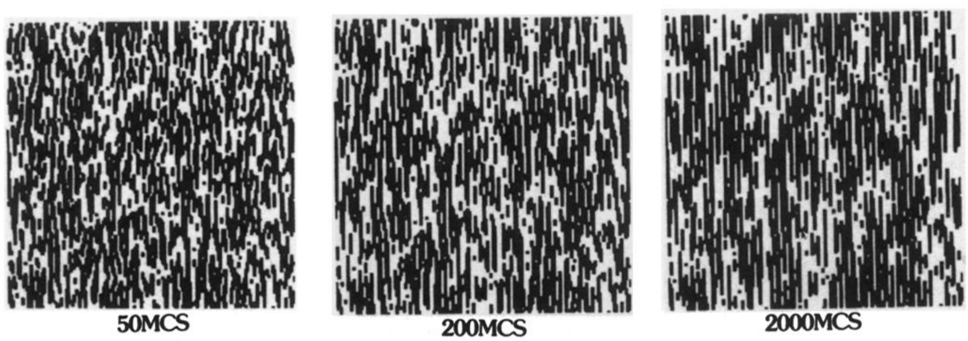

FIG. 9. The temporal evolution of the ANNNI microstructure following a quench from $T \gg T_c$ to $T = 0.02$ for $\kappa = 0.08$.